Poly (Acrylic Acid-Co-Styrene)/HDTMA-MMT Composite for Efficient Adsorption of Phenol Wastewater: Isotherm and Kinetic Modeling

Djamaa, Zoulikha[*+•]

Center for Scientific and Technical Research in Physico-Chemical Analyzes (CRAPC). Industrial Zone No. 30, Bou-Ismail, Tipaza , ALGERIA

Louahla, Hadjer; Guemra, Kaddour

Laboratory of Organic Chemistry, Physical and Macromolecular (LCOPM). University of Sid Bel-Abbès, Department of Chemistry, Sid Bel-Abbès, ALGERIA

Bachari, Khaldoun, Lerari, Djahida[••]

Center for Scientific and Technical Research in Physico-Chemical Analyzes (CRAPC). Industrial Zone No. 30, Bou-Ismail, Tipaza, ALGERIA

ABSTRACT: *A composite, based on poly (acrylic acid-co-styrene) and organomodified montmorillonite with hexadecyltrimethyl ammonium bromide (27 wt. % in inorganics), designated as: poly(AA-co-St)/HDTMA-MMT was prepared by in situ radical polymerization. The structural and morphological properties were examined by Fourier transform infrared (FTIR) spectroscopy, X-Ray Diffraction (XRD), and scanning electron microscopy (SEM). The results show the intercalation of poly (acrylic acid-co-styrene) in the organomodified montmorillonite layers. The percent of the inorganics in the composite is 27 % as evaluated by ThermoGravimetric Analysis (TGA). The performance of the composite to remove phenol molecules from an aqueous solution was investigated by batch adsorption, under different experimental conditions. The zeta potential of poly(AA-co-St)/HDTMA-MMT composite was calculated to understand the mechanism of phenol adsorption onto poly(AA-co-St)/HDTMA-MMT. The pollutant uptake behavior was determined by UV-Vis spectrophotometry. The best results were obtained for a contact time of 180 minutes, an initial concentration of 30 mg/L, pH 6. The presence of acrylic acid and styrene can modify the surface characteristics of the composite and affect the adsorption capacity as confirmed by X-Ray Diffraction (XRD) and Scanning Electron Microscopy (SEM). Interestingly, the maximum adsorption capacity was found to be 150.7 mg/g. Equilibrium modeling*

* To whom correspondence should be addressed.

+ E-mail: z_djamaa@yahoo.fr

• Other Address: Laboratory of Organic Chemistry, Physical and Macromolecular (LCOPM). University of Sid Bel-Abbès, Department of Chemistry, Sid Bel-Abbès, ALGERIA

•• Other Address: Laboratory of Macromolecular and Thio-organic Macromolecular Synthesis, Faculty of Chemistry, University of Sciences and Technology Houari Boumediene, USTHB, Algiers, ALGERIA

of the phenol removal process was carried out using the Langmuir and Freundlich adsorption isotherms. The equilibrium adsorption data were found to be well-fitted with the Freundlich adsorption isotherm. The kinetic of adsorption was best described by a pseudo-second-order expression rather than a first-order model. The interactions between phenol molecules and adsorbent were explained by electrostatic as well as hydrogen bonding interactions, as confirmed by the pseudo-second-order kinetic model. A model for the interactions between a composite and phenol molecule was proposed. Interestingly, the desorption of phenol from the adsorbent using hot water remains stable. The value of the first adsorption/desorption cycle was about 98.1 % and achieved 92.8 % after five cycles.

INTRODUCTION

Wastewater containing organic contaminants such as phenolic compounds implies the presence of serious problems associated with its discharge to the surrounding environment, this is primarily owing to their poor biodegradability, high toxicity, and possible accumulation in the environment [1]. The rapid increase in organic waste generated from various industries and other sources in recent decades has resulted in the widespread distribution of organic pollutants in the hydrosphere [2]. Phenol is harmful to organisms even at low concentrations. Therefore, it is classified as a potentially dangerous pollutant for human health [3]. Phenolic compounds are generally produced as side-products resulting from various chemical reactions in the industry, e.g., the production of dyes, aspirin synthesis, paper, etc. Phenol is found to be toxic at very small levels; the molecule is found to produce an unpleasant smell in water and is capable of reacting with chlorine and/or NO_2 in the soil to produce other harmful substances such as chlorophenol and nitrophenol. Most authorities impose a value of 1 ppm as the maximum limit of phenol present in wastewater [4, 5]. Exposure to phenol and its derivative compounds causes liver and kidney damage, central nervous system impairment, diarrhea, and dark urine production in humans and animals [6, 7]. Therefore, it is necessary to develop methods that allow one to detect, quantify, and remove phenol from wastewater [8]. Because phenol is highly stable and water-insoluble, its degradation is low. Phenol and phenolic compounds have half-lives ranging from 2 to 72 days [9]. Phenolic compounds have toxic effects on human and aquatic life. Consequently, their permitted limits are low (0.5-1.0 mg/L), thus making its removal

from wastewater using appropriate methods a necessity [10,11]. Numerous researchers have investigated methods to remove organic pollutants from aqueous phases e.g., catalytic oxidation [12, 13], electrochemical decomposition [14], solvent extraction [15], ion exchange [16], and adsorption [17-20]. However, adsorption is considered the most effective and economical method used for removing pollutants. For this, many adsorbents have been used to remove phenol from aqueous solutions such as organobentonite [21, 22], activated carbon [23], heterostructural porous clay [24], and chitosan [25, 26].

Clay is a natural substance consisting primarily of fine grain rocks, which can be plastic and water content sufficient to harden when dried and fired. Clays are hydrous aluminosilicates, which are commonly described as pyrophyllite-talk, smectite-montmorillonite, mica-illite, kaolinite, serpentine, vermiculite, and sepiolite minerals in different categories [27]. Kaolinite has a small net negative charge, due to the presence of broken edges on the clay crystals. Although small, this negative charge is responsible for the surface not being completely inert [28, 29]. The chemical alteration may increase the adsorption potential of clay, leading to its widespread use in new technologies. The effectiveness of clay in adsorption is usually based on the net negative charge found on clay minerals. The negative charge contributes to the ability of clay to absorb positively charged ions. The adsorption properties of clays are derived from their large pore size and surface area [30]. Generally, clays have interchangeable ions on their surface, which play a crucial role in the uptake of chemical pollutants [31]. So, new challenges are being faced in the development

of adsorbent materials that can cover the expectations of sustainability and maximum efficiency in the processes of wastewater treatment [32].

Polymer/clay composites are considered promoter materials in this field of research [33]. These composites are classified according to the interaction between the polymer matrix and the silicate layer filler [33-41]. Significant improvements in physical properties such as heat resistance [42, 43], biodegradability [44], air permeability [45], and flammability [46] were demonstrated. The in situ polymerization method is the most commonly used method for preparing polymer/clay composites. The organoclay is combined with the monomer instead of the polymer, resulting in well-dispersed and homogeneous composites. The intercalated structure is formed by the intercalation of the polymer chains between the clay layers and this results in increasing the value of the interlayer spacing. In the intercalated structure, the clay preserves the same order, and crystallinity can be observed [36]. The abundance of clay minerals in the World and its low cost make it a potential adsorbent for the removal of many pollutants from wastewater. Clay minerals are not efficient as an adsorbent for the uptake of hydrophobic organic pollutants from aqueous solutions. But polymers-clay which are produced by *in situ* intercalative polymerization of polymer chains into clay layers have enhanced sorption capacities for organic pollutants.

Acrylic acid is an unsaturated carboxylic acid consisting of a vinyl group linked to the carboxylic acid junction [47]. The interesting solubility profile of this superabsorbent enables the removal of dyes, and heavy metals under different solution conditions. Many researchers have documented the use of poly (acrylic acid)-based composites to remove organic pollutants [48, 49], safranine T [50], and metal ions like zinc, nickel, magnesium copper, and lead [51, 52]. Several techniques have been reported to prepare poly(acrylic acid) [18, 53, 54]. *Rahman et al.* [47] described the removal of methylene from wastewater/aqueous solution using a modified clay-grafted poly(acrylic acid) polymer. *Moon et al.* [55] studied the adsorption of phenol, *p*-chlorophenol, and *p*-nitrophenol adsorption on polystyrene crosslinked divinyl benzene. *Hernandez et al.* [32] used alginate beads, with an organo-modified montmorillonite with hexadecyltrimethylammonium ions for the removal of

phenol and 4-chlorophenol from aqueous solutions. *Biswas et al.* [56] synthesized chitosan-modified clay biocomposite beads and evaluated their applicability in removing Pb(II) and methylene blue dye from a standard model solution. In addition, as a preliminary study, the efficiency and performance of these composites in the removal of Cr(VI), Pb(II), and methylene blue (MB) from two real industrial effluents were investigated. Recently, *Bhatia et al.* [57] explored the use of poly(acrylic acid)/clay hydrogel as an adsorbent of lead ions and optimized physicochemical parameters influencing the adsorption process. In our previous work, poly(acrylic acid-*co*-styrene)/clay nanocomposites were synthesized, and their efficiency as adsorbents of the methylene blue dye was evaluated [58]. As far as we know, there are no studies in the literature reporting the removal of phenol into Poly(acrylic acid-co-styrene)/Montmorillonite-hexadecyltrimethyl ammonium bromide (poly(AA-co-St)/HDTMA-MMT) Composite.

This work aims to highlight the efficient potential adsorption of the poly(acrylic acid-*co*-styrene)/Montmorillonite-hexadecyltrimethyl ammonium bromide composite (27 wt. % in inorganics) for the phenol wastewater treatment. The poly(AA-co-St)/HDTMA-MMT composite was characterized by different techniques, then tested as an adsorbent for the sorption of phenol from an aqueous solution *via* a batch adsorption experiments. The adsorption, kinetics, and isothermal analyses were examined. The equilibrium adsorption data were fitted with the Langmuir and Freundlich adsorption isotherms. To predict the adsorption kinetics, various kinetics models, namely the pseudo-first and pseudo-second orders, were applied to explain our findings.

EXPERIMENTAL SECTION
Materials

The monomers acrylic acid (AA) (Aldrich Chemical, 98%) and styrene (St) (Aldrich Chemical, 98%) were distilled under reduced pressure prior to use. The free radical initiator,2, 2'-azobis (isobutyronitrile) (AIBN) (Aldrich, 98%) was purified by recrystallization in methanol. Hexadecyltrimethyl ammonium bromide (HDTMA-Br) (Aldrich, 99%) was used without further purification. Toluene and heptane (Aldrich Chemical)
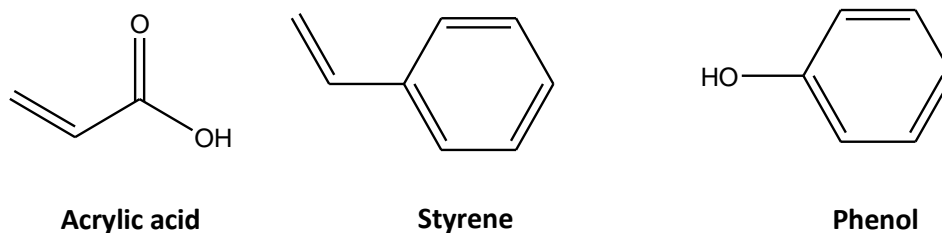
Acrylic acid　　　　**Styrene**　　　　**Phenol**

Fig. 1: Chemical structure of reagents

distilled under reduced pressure prior to use. The free radical initiator,2, 2'-azobis (isobutyronitrile) (AIBN) (Aldrich, 98%) was purified by recrystallization in methanol. Hexadecyltrimethyl ammonium bromide (HDTMA-Br) (Aldrich, 99%) was used without further purification. Toluene and heptane (Aldrich Chemical) were used after distillation. The Algerian clay (MMT) used in this study was natural montmorillonite from Mostaganem (Algeria), kindly supplied by Enterprise Nationale des Produits Miniers Non-Ferreux et des Substances Utiles (ENOF), Algeria. MMT chemical composition $(Si_{4.24})^{IV}(Al_{1.24} Mg_{0.2} Fe_{0.17} Ti_{0.01})^{VI} O_{10}$ $(OH)_2$, nH_2O $Na_{0.13}$, $Ca_{0.01}$, $K_{0.1}$ was reported by the supplier. The organic pollutant used in this study is phenol (Cheminova International S.A). The chemical structure of all reactants is depicted in Fig. 1.

Montmorillonite organo-modification: HDTMA-MMT

Firstly, the natural clay was dispersed in an aqueous solution, and the organic impurities were eliminated by treatment with hydrogen peroxide. Then, montmorillonite (MMT) was converted into its sodic form by reaction with NaCl. Finally, the organophilic form of MMT was obtained by ion-exchange reaction of the Na^+cations with HDTMA as reported elsewhere [58, 59] and freeze-dried for about 12h. The obtained organomodified clay is denoted as HDTMA-MMT.

Synthesis of adsorbent: poly (acrylic acid-co-styrene)/ HDTMA-MMT: poly(AA-co-St)/HDTMA-MMT

The synthesis of composite poly(acrylic acid-*co*-styrene)/HDTMA-MMT is similar to the one described in our earlier work [58], except that the initial inorganic content in the polymer composite was fixed at 30 wt.%. Briefly, distilled acrylic acid and styrene monomers, AIBN (0.1 wt.%) and HDTMA-MMT (30 wt.%) in toluene were placed in the reactor and stirred at room temperature under nitrogen flow for a few minutes.

The copolymerization was carried out for 8 h, at 70 °C. The polymerization reaction was stopped by a quick decrease in the reactor temperature. The obtained composite, abbreviated as poly(AA-*co*-St)/HDTMA-MMT, was recovered by precipitation/filtration and drying under vacuum for 30 h.

Determination of isoelectric point pH_{PZc}

The pHpzc of poly(AA-*co*-St)/HDTMA-MMT was determined by a previous method cited in the literature [60]. A solution of KCl (0.001 M) was transferred to a series of Erlenmeyer flasks which was made up of exactly 25 mL. The initial pH of each flask was adjusted by adding either HCl (0.1 M) or NaOH (0.1 M). The composite (25 mg) was added to each flask. After 48 h of stirring, the suspensions were filtered and the final pH values of the supernatant liquid (pH_{final}) were recorded. The pHpzc is the point where the curves of final pH versus initial pH cross the axis line of the bisectors.

Batch adsorption experiments

For the batch adsorption study, 40 mg of the synthesized composite poly (AA-*co*-St)/HDTMA-MMT was placed in contact with 10 mL phenol solution at ambient temperature for 300 min. [47] The concentration of phenol solution was varied from 30 to 600 mg/L. After shaking the mixture was allowed to settle and a small volume of the sample was separated from the top of the settled solution for determining the concentration of phenol. The concentration of the adsorbed pollutant was evaluated by UV-visible at a wavelength λ = 270 nm, according to the Beer-Lambert Equation (1)

$$A = \varepsilon\, l\, C \tag{1}$$

Where A is the absorbance, ε (L/mol.cm) is the molar absorption coefficient (ε = 1 L/mol.cm), C (mol/L) is the molar concentration and l is the optical path length (cm). The amount of fixed pollutant per gram of adsorbent
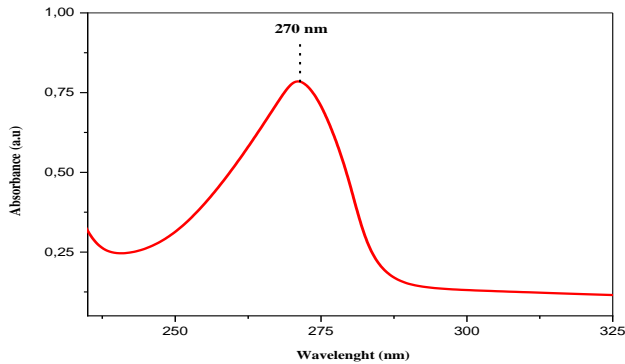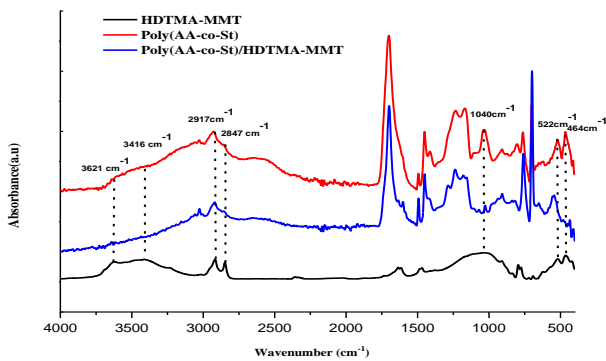
Fig. 2: UV-visible spectrum of phenol pollutant

Fig. 3: FT-IR spectra of the modified clay, synthesized copolymer, and composite poly (AA-co-St)/HDTMA-MMT

is calculated using the following equation [18]:

$$q_t = \frac{(C_i - C_f)V}{m} \tag{2}$$

Where C_i and C_f are the initial and equilibrium concentrations of phenol, respectively. *V* is the volume (L) of the phenol solution and m (g) is the weight of the used adsorbent.

Recovery experiment

The adsorbent, poly (AA-*co*-St)/HDTMA-MMT composite, at the concentration of 4 gL^{-1} was saturated with 30 mg/L phenol solution for 12 hours. On drying, the adsorbent was subjected to hot water treatment for a period of 24 hours. The amount of phenol sequestered in water accounted for the percent desorption and was calculated using the formula:

$$\text{Desorption (\%)} = \left[\frac{q_{des}}{q_{ads}}\right] \times 100 \tag{3}$$

$$q_{des} = C_{des}\frac{V}{m} \tag{4}$$

Where q_{des} is the content of desorbed phenol (mg/g), C_{des} (mg/L) is the concentration of phenol in the solution

with volume *V* (L) and m is poly (AA-*co*-St)/HDTMA-MMT weight (g). [23]

Instrumentation

Fourier Transform Infrared spectra with Attenuated Total Reflectance (FTIR-ATR) of the modified clay and the synthesized composite were conducted in absorption mode using a spectrophotometer ALPHA-BRUKER, at a resolution of 4 cm^{-1}, with 32 scans, in the range of 4000–400 cm^{-1}. The X-Ray powder Diffraction (XRD) analyses of all materials were performed using a BRUKER D8 ADVANCE diffractometer with CuKα radiation (λ = 0.15406 nm) from 1.65° to 30° by step of 0.04° and a scanning rate of 10°/min. The clay content in the synthesized composite was evaluated by thermogravimetric analysis (TGA) using a thermal analysis calorimeter (SDT Q600, TA instrument), in an aluminum cell under nitrogen flow at a rate of 20 K.min^{-1}, from room temperature to 800℃. The surface morphology of the composite was examined using Quanta 250 Scanning Electron Microscopy (SEM), equipped with a field emission filament with an acceleration voltage of 5 kV and a working distance of 10 mm. The point of zero charges of poly(AA-co-St)/HDTMA-MMT composite was determined using a potentiometer COMBO by HANNA. The phenol retention content was evaluated according to a UV-visible spectrophotometer SPECORD 200 Analytica Jena. The calibration plot was defined according to the change in absorbance values of the phenol solution of a known concentration at λmax = 270 nm (Fig. 2).

RESULTS AND DISCUSSION
### *Characterization of adsorbent polymer composite*
Fourier transform infrared spectroscopy analysis
a) Fourier transform infrared spectroscopy analysis of poly (AA-co-St)/HDTMA-MMT

FTIR spectra of organo-modified clay, the synthesized copolymer, as well as the corresponding composite, are depicted in Fig. 3. The FT-IR spectrum of the modified clay demonstrates the presence of principal bands of the nano-filler. The bands centered around 3621 cm^{-1} and 3416 cm^{-1} are assigned to the stretching vibrations of hydroxyl groups existing in the modified clay. The peak at 1040 cm^{-1} defines the stretching vibrations of Si-O, Si-O-Si, and Al-O bonds [59]. The peaks recorded at 522 cm^{-1} and 464 cm^{-1} are the result of deformation vibrations of Al-O and Mg-O

Table 1: IR spectra of poly (AA-co-St)/HDTMA-MMT before (A) and after (B) phenol adsorption

	-OH (cm^{-1})	Si-O, Si-O-Si (cm^{-1})	Al-O (cm^{-1})	Mg-O (cm^{-1})
A	3621	1040	522	464
B	3613	1006	513	457
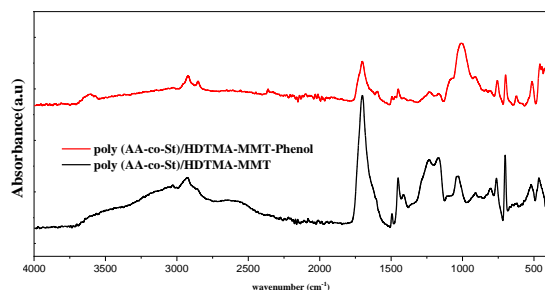
Fig. 4: FTIR spectra of composite poly (AA-co-St)/HDTMA-MMT before and after phenol adsorption
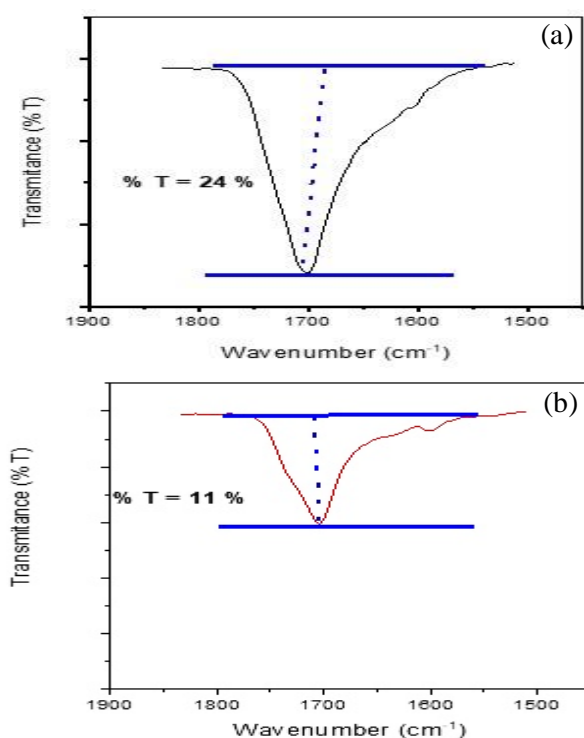
Fig.5: The comparison of the change in intensity of C=O stretching mode of PAA in (a) poly (AA-co-St)/HDTMA-MMT and (b) poly (AA-co-St)/HDTMA-MMT-phenol

groups, respectively. The peaks at 2917 cm^{-1} and 2847 cm^{1} are assigned to the stretching vibrations of the alkyl groups and confirm the success of the clay organo-modification reaction. For the synthesized copolymer, the principal

bands of functional groups are detected. Especially, the band at 1700 cm^{-1} which is assigned to the carboxylic group of the acrylic acid [40]. The bands showing stretching vibrations of the styrene phenyl group were recorded at 1456 cm^{-1}, 755 cm^{-1}, and 701 cm^{-1} [20]. Interestingly, the principal bands of poly (AA-*co*-St), as well as those of HDTMA-MMT, were detected in the poly (AA-*co*-St)/HDTMA-MMT FT-IR spectrum, implying the formation of the polymer composite.

b) Fourier transform infrared spectroscopy analysis of poly (AA-co-St)/HDTMA-MMT-phenol

The FTIR spectra of poly (AA-co-St)/HDTMA-MMT before and after phenol adsorption were used to determine the vibrational frequency changes in the functional groups in the adsorbent (Table 1). As shown in Fig.4, the adsorption peak around 3613 cm^{-1} indicates the existence of free hydroxyl groups. The shifting of the peaks (from 3621 cm^{-1}, 1037 cm^{-1}, 522 cm^{-1}, and 464 cm^{-1}) was noticed after phenol adsorption, as illustrated in Fig.4 and Table 1. According to these findings, the functional groups (-OH, -CO, -Si-O and O-Si-O, Al-O and Mg-O) at these wave numbers have contributed to the phenol adsorption [61]. The intensity of C=O stretching at 1700 cm^{-1} decreased from 24% to 11% as demonstrated in Fig.5. This might be explained by the hydrogen bond formed by the interaction of the hydroxyl group in phenol with the hybrid polymer matrix at the oxygen atom of the carboxylic group (C=O), which has two lone pairs of electrons [62].

X-ray diffraction characterization

The formation of the composite was also confirmed by XRD analysis. Therefore, the structural characterization of the clay before and after organo-modification was illustrated in the XRD patterns of MMT and HDTMA-MMT (Fig. 6.). Based on Bragg's equation, the 001 plan peak of MMT, initially centered at $2\theta = 6.65°$, was found to shift towards lower 2θ values after the organo-modification reaction ($2\theta = 3.95°$), implying an increase in the interlayer spacing from 13.24 Å to 23.67Å [59]. According to *Ltifi et al.* [63], the theoretical length of the HDTMA cation is 25.3 Å, the height of the alkyl chain is 4.1 Å, and the head of the nail is 5.1 Å; The HDTMA cation is flat between layers of montmorillonite. The difference between the values of the basal space d001, as observed by an increase in interlayer space from13.24 Å to 23.67Å, is due to the organization of the alkylammonium ions (HDTMA)
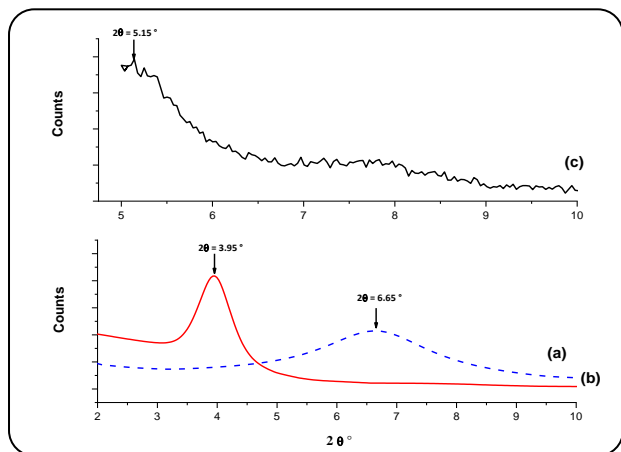
Fig. 6: XRD patterns for MMT (a), HDTMA-MMT (b) and poly (AA-co-St)/HDTMA-MMT (c)

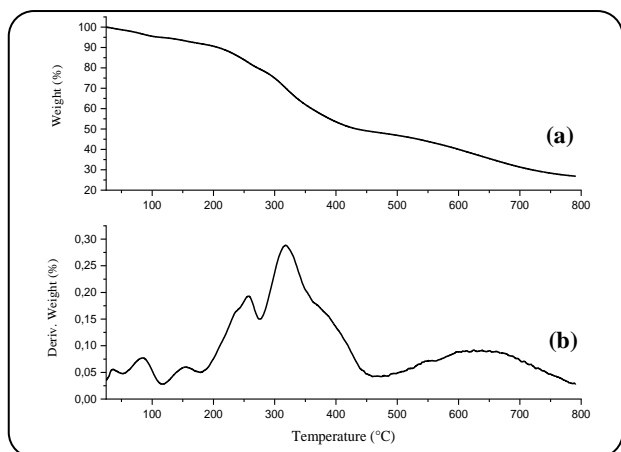

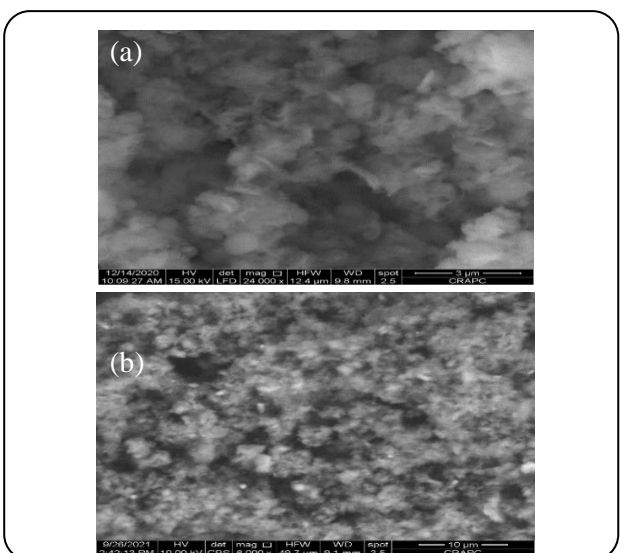**Fig. 7: TGA(a) and DTG(b) thermograms of poly (AA-co-St)/HDTMA-MMT, in the air at a heating rate of 20 K.min⁻¹**

Fig. 8: SEM images of synthesized poly (AA-co-St)/HDTMA-MMT (A) at ×24 000, (B) at ×6000 magnification

in the interfolliairy space. In our case, the alkyl chains adopt an inclined paraffin-type monolayer structure. Therefore, the type of arrangement depends on the length of the alkyl chain and the basal space d001 value. The composite prepared by *in-situ* radical polymerization was also characterized and the diffraction peaks were recorded at approximately $2\theta = 5.15°$, indicating some collapse of the nanoclay platelets, possibly due to the alkyl group HDTMA-Br left the montmorillonite interlayers during the *in situ* radical polymerization.

Thermogravimetric analysis

The TGA and DTG curves of poly(AA-*co*-St)/HDTMA-MMT, conducted under airflow, are shown in Fig. 7(a) and Fig. 7(b) respectively. A loss of adsorbed water was observed between 35°C and 154°C. The surfactant thermodegradation was achieved at around 257°C, followed by the copolymer degradation in the range [276°C - 455°C]. The dehydroxylation of clay started at 529°C. Indeed, the percentage of inorganics in the synthesized poly(AA-*co*-St)/HDTMA-MMT was evaluated at about 27 wt.%, in accordance with the experimental conditions.

Scanning electron microscopy

The morphology of the synthesized composite was examined according to SEM images (Fig. 8A) at ×24 000, and at ×6000 magnifications. (Fig. 8B). The images revealed that the surface of the composite was irregular. The color of the composite was black. At ×24 000, and at ×6000 magnifications, SEM micrographs of the adsorbent revealed rough surface morphology, indicating heterogeneity and therefore offering better adsorption sites. The SEM study of the composite sample at higher magnification showed that there were bright globular particles, and the surface of the composite displayed some brilliant closings which can be evaluated as poly(AA-*co*-St)/HDTMA-MMT. Fig. 8. indicates that the montmorillonite particles were dispersed throughout the copolymer matrix.

Determination of isoelectric point pHpzc

The pH at which the charge of the adsorbent surface is zero is referred to as the point of zero charges (pHpzc). The pHpzc is one of the important parameters for the discussion of the pH effect. When solution pH values are lower than pHpzc, the active sites of the adsorbent are protonated and have a positive charge. However, when
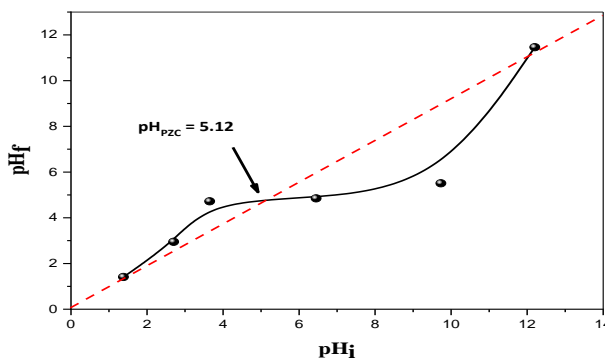
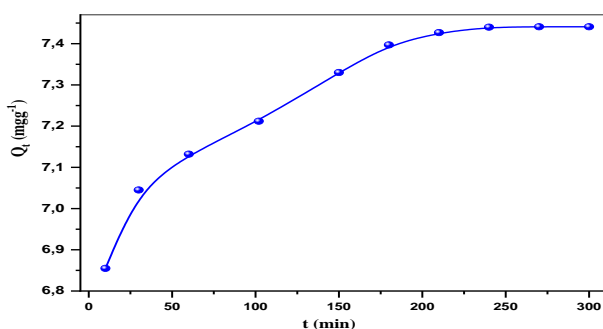**Fig. 9: Point of zero charge of poly (AA-co-St)/HDTMA-MMT composite**

Fig. 10: Kinetics of phenol uptake on poly (AA-co-St)/HDTMA-MMT: pH = 6, initial phenol concentration 30 mg.l⁻¹, T = 293 K
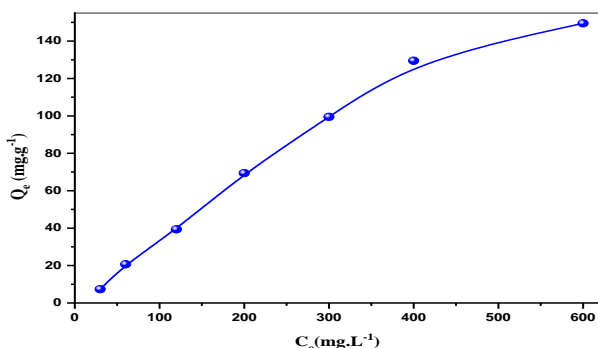

Fig. 11: Isotherm of phenol adsorption on poly (AA-co-St) /HDTMA-MMT (pH = 6, t=180 min, T = 293 K)

pH values are higher than pHzpc, the surface charge of the adsorbent is negative. In all our adsorption experiments we opted to work at a pH higher than 5.12 (pH ≈ 6) so that the surface was negatively charged and we would have more interactions between the adsorbent and phenol (Fig. 9).

Adsorption study
Effect of contact time on phenol adsorption

Fig. 10 shows the variation of adsorbed phenol (mg/g)

as a function of time (min). Generally, the pollutant transfer from the liquid phase to the solid phase governs the adsorption, which is dependent on the contact time between the two phases. In our case, the phenol removal was firstly conducted as a rapid adsorption step which is achieved after 180 min of contact, followed by a saturation phase (Fig. 10). As reported in the literature by *Banat et al.* [64], the equilibrium time required for the adsorption of phenol on bentonite was about 6 h**.** In other works, published by *Lin et al.* [64], the equilibrium time was achieved after 34 h of contact when poly (methylmethacrylate)/organo-montmorillonite composite was used**.** Also, a maximum phenol removal capacity of 0.377 mgg⁻¹ was recorded using alginate-organo-modified clay, with an equilibrium time of 9 h as described by *Hernández-Hernández et al.* [32]. This significant finding emphasizes the importance of the selected copolymer as the organic phase and clay as the inorganic phase on the synthesized composite for improving phenol pollutant adsorption.

Effect of phenol initial concentration

Fig. 11. highlights the evolution of phenol adsorption (mg/g) as a function of solution initial concentration (mg/L) with a contact time of 180 min. The adsorbed phenol molecules on poly(AA-*co*-St)/HDTMA-MMT increased with increasing the concentration of pollutants in the solution. This may be attributed to the increase of mass transfer driving force and therefore the transport rate of phenol molecules from the solution to the adsorbent composite. As shown in Fig. 11, the isotherm plot is illustrated as a regular and concave profile that is classified as L-type according to Giles' classification [66, 67]. The phenol pollutant showed a high affinity toward the composite adsorbent. Interestingly, the maximum adsorption capacity of phenol on the studied composite was 150.7 mg/g, with a phenol removal efficiency of 96.6 %, which is superior to the reported results [32, 65, 68]. *Hernández et al.* [32] investigated the removal of phenol and 4-chlorophenol on alginate/organo-modified clays nanocomposite and reported maximum removal capacities values of 0.334 mg/g and 0.118 mg/g for phenol and 4-chlorophenol, respectively. *Yagmur et al.* [68] studied the adsorption of 4-nitrophenol on polypyrrole/bentonite nanocomposite. The maximum adsorption capacity was defined as 96.15 mg/g at 298 K. In addition, for the *p*-nitrophenol pollutant, a maximum adsorbed amount of

Table 2: Adsorption performance of various adsorbents regarding phenol pollutant

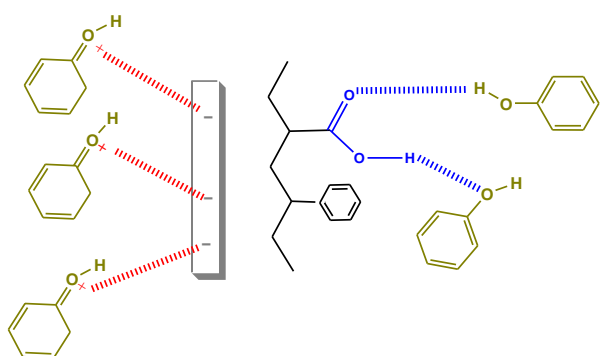| Adsorbents	Pollutants	Adsorption capacity (mg/g)	Ref.
Lignite	Phenol	10	[10]
CTAB-MMT	phenol	9.1	[11]
Organo-bentonite	phenol	81.36	[22]
Na-bentonite	Phenol	21.96	[24]
Ca-bentonite/chitosane	phenol	12.49	[26]
Alginate/OMMT	Phenol	0.33	[32]
Bentonite	Phenol	1.71	[64]
PMM/OMMT	p-nitrophenol	3.8	[65]
PP/OMMT	4-nitrophenol,	96.15	[68]
poly(AA-co-St)/HDTMA-MMT	phenol	150.7	This work

Fig. 12: Proposed interactions of phenol pollutant with poly (AA-co-St)/HDTMA-MMT adsorbent

3.8 mg/g was obtained after 34 h, using porous poly (methyl methacrylate)/organo-montmorillonite composite membranes, as reported by *Lin et al.* [65]. In our case, the synthesized composite showed higher adsorption capacity toward phenol as compared to those reported in the literature [10, 11, 22, 24, 26, 32, 64, 65, 68]. This is probably associated with the diversity of interactions, which can be developed between the pollutant and the adsorbent matrix. As shown in Fig. 12., two types of interactions can be considered: electrostatic and H-bonding interactions. The electrostatic attraction was found to result from the negatively charged surface of the modified clay caused by the pH of the solution (pH= 6) and the electronic doublet of oxygen of the hydroxyl function of the pollutant molecule. It is important to note that the important content of inorganics in the adsorbent composite (27 wt.%) increases the number of sites involved in these electrostatic interactions. On the other hand, hydrogen bondings were formed between the hydroxyl groups of the phenol molecules and the carboxylic functional group of acrylic acid co-monomer,

leading to an improvement in phenol uptake. Table 2 presents a summary of the adsorption capacity of some adsorbents. The poly (AA-*co*-St)/HDTMA-MMT offered the best performance for phenol removal.

Adsorption isotherms modeling

Equilibrium studies provide information on the adsorption capacity of the adsorbent; therefore, they are necessary to complete the understanding of the adsorbent. An adsorption isotherm is characterized by some constant values, which express the surface properties and the affinity of the adsorbent and can be used to compare the adsorptive capacities of the adsorbent for different pollutants. Several mathematical models can be used to describe the experimental data of adsorption isotherms. The Langmuir and Freundlich models are used to fit the adsorption isotherms and to evaluate the isotherm parameters [1].
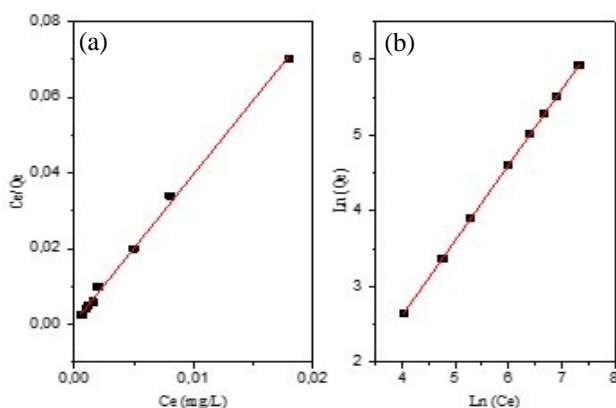
Langmuir isotherm

The Langmuir isotherm considers several assumptions: the adsorption is localized, all the active sites on the surface have similar energies, there are no interactions between adsorbed molecules, and the limiting reaction step is the surface reaction [1]. The Langmuir equation was derived for the sorption of gases on the solid surface. Nevertheless, it has been extended to include the sorption of solute at a solid-liquid interface. The Langmuir isotherm is valid for monolayer adsorption onto the surface containing a finite number of identical sites [68]. The linearize of the Langmuir model is defined as follows:

$$\frac{C_e}{Q_e} = \left(\frac{1}{bQ_m}\right) + \left(\frac{C_e}{Q_m}\right) \tag{5}$$

Table 3: Langmuir and Freundlich coefficients for adsorption of phenol on poly (AA-co-St)/HDTMA-MMT (m= 40 mg, V= 10 mL, pH= 6, t=180 min)

Model	Parameters	value
Langmuir	Q_m (mg/g)	200
	b (L/g^{-1})	0.01
	R^2	0.982
Freundlich	n	1.012
	1/n	0.988
	K (mg$^{1-(1/n)}$ L$^{1/n}$g^{-1})	1.47
	R^2	0.999
$Q_{max,exp}$ (mg/g)	--	150.7

Fig. 13: Adsorption isotherm of phenol using Langmuir (a) and Freundlich (b) equations obtained for poly (AA-co-St)/HDTMA-MMT. (m= 40 mg, V= 10 mL, pH= 6, t=180 min)

Where; Q_e: the adsorption capacity of the adsorbate per unit weight of adsorbent (mg/g), Q_m: the maximum adsorption capacity (mg/g), b: the constant related to the free energy of adsorption (L/mg), and Ce is the equilibrium concentration of the adsorbate (mg/L) [69].

A graphic plot of Ce/qe versus Ce indicates a straight line of slope $1/Q_m$ and intercept of $1/Q_mb$ [70]. The fitting of the Langmuir model to the experimental phenol removal data is illustrated in Fig. 13(a). The parameters for linear Langmuir isotherms are summarized in Table 3. The Langmuir model results are not in accordance with the experimental one.

Freundlich isotherm

The Freundlich model is an empirical equation that describes the equilibrium of sorption on heterogeneous surfaces through a multilayer adsorption mechanism [71, 72]. It is calculated according to Equation (6).

$$Q_e = K_N C_e^{1/n} \qquad (6)$$

Where; Q_e: Equilibrium amount of the adsorbate per unit mass of adsorbent (mg.g^{-1}), C_e: Equilibrium concentration of the adsorbate (mg.L^{-1}), K_N is a constant that indicates the adsorption capacity of the adsorbent at the unit concentration (mg/g) (L/mg)$^{1/n}$ while $1/n$ indicates the intensity of the adsorption.

The values of k and n can be obtained from the intercept and slope, respectively, of the linear plot of experimental data of Ln Qe versus Ln C_e.

The linearized form of the Freundlich model is:

$$LnQ_e = Ln\ k + n\ Ln\ C_e \qquad (7)$$

Where k and n are model constants showing the relationship between adsorption capacity and adsorption intensity, respectively. If the Freundlich constant n lies between 1 and 10, it indicates a favorable adsorption process and a larger value of n implies the effective interaction between the adsorbent and adsorbate [73,74]. The Langmuir and Freundlich adsorption parameters are determined by plotting the experimental data based on Equations 5 and 7, respectively (Fig.s 13a,13b). The determined parameters and their corresponding correlation coefficients (R^2) are listed in Table 3. As seen in Fig. 13(b) and Table 3, the Freundlich equation confirmed our adsorption model by the presence of a correlation coefficient value ($R^2 = 0.999$). Furthermore, the slope of 1/n ranging between 0 and 1 is a measure of the adsorption intensity or surface heterogeneity, this value becoming more heterogeneous as it approaches zero. A value for 1/n below one indicates a normal Freundlich isotherm while a 1/n value above one is indicative of cooperative adsorption. In this study 1/n value of 0.988 confirms the Freundlich isotherm [72] and surface heterogeneity shown by the characterization. Moreover, the results in Fig. 14 indicate that the Freundlich isotherm best fits the experimental data for phenol adsorption on poly (AA-co-St)/HDTMA-MMT. In this Fig., the theoretical plots for all isotherms have been compared with the experimental data.

Kinetics modeling

In order to examine the kinetic of solid-liquid interactions in our system, two kinetic models based on adsorption capacity were proposed: the pseudo-first-order

Table 4: Parameters values of pseudo-first-order and second-order models for adsorption of phenol on poly (AA-co-St)/HDTMA-MMT (Initial phenol concentration 30 mg.l⁻¹, m= 40 mg, V= 10 mL, pH= 6, T= 293 K)

Kinetics models	Parameters	value
Pseudo-first-order	Q_e (mg/g)	8.4
	k_1 (min⁻¹)	0.01
	R^2	0.842
Pseudo-second-order	Q_e (mg/g)	7.1
	k_2 (g mg⁻¹min⁻¹)	0.113
	R^2	0.999
$Q_{e,exp}$ (mg/g)	--	150.7
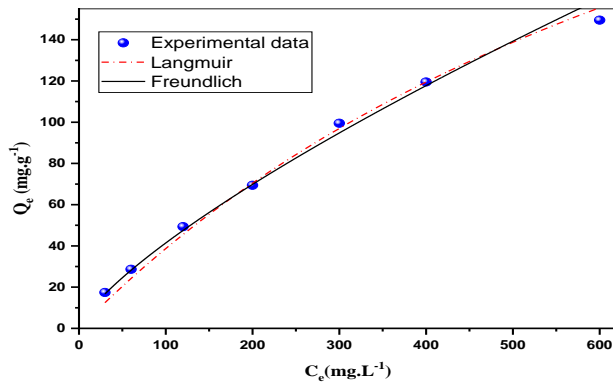
Fig. 14: Comparison of the adsorption equilibrium isotherms of phenol onto poly (AA-co-St)/HDTMA-MMT with the experimental points
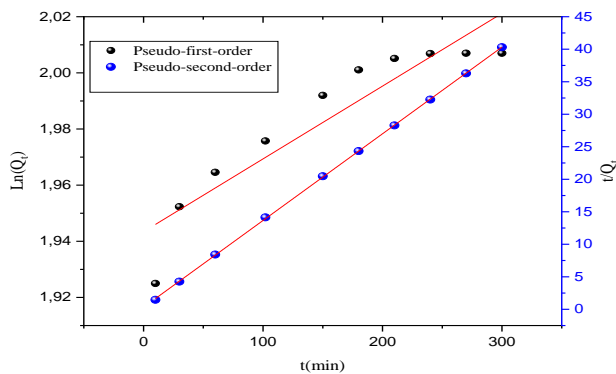
Fig. 15: Pseudo-first-order and Pseudo-second-order adsorption kinetics of phenol adsorption on poly (AA-co-St)/HDTMA-MMT (m= 40 mg, V= 10 mL, pH= 6, T= 293 K)

and the pseudo-second-order models (Fig. 15). In the case of the first model, diffusion and mass transfer of the adsorbate to the adsorption site govern the overall process. For the pseudo-second-order kinetic model, chemisorption is the rate-limiting step [47]. The linearized-integral form of the most popular pseudo-first-order model (Eq. (10)) [75] by Lagergren is the integrated form (Eqs (8) and (9)) of the pseudo-second-order model [76] of the following

equations:

$$\frac{dq_t}{dt} = k_1(q_e - q_t) \tag{8}$$

$$q_t = q_e (1 - e^{-k_1 t}) \tag{9}$$

$$\ln(q_e - q_t) = \ln q_e - k_1 t \tag{10}$$

Where k_1 is the pseudo-first-order rate constant of the adsorption process (min⁻¹). The values of q_e and k_1 are calculated by the non-linearized form Equation (8), and the value of R^2 is carried out by the linearized form Eq. (10). The equation parameters of the two kinetic models are summarized in Table 4. From the table, it can be seen that the experimental data fit well with the pseudo-second-order model with an R^2 value higher than that of the pseudo-first-order model; the adsorption of phenol on our composite followed the pseudo-second-order model, which demonstrated that the adsorption should be a physisorption process [77,78]. Based on the above experimental observations with the kinetic and equilibrium isotherm parameters, the chemical interactions with phenol are primarily responsible for the adsorption behavior based on the analysis of the pseudo-second-order model. These results confirm the suggested interactions governing the phenol uptake in presence of poly(AA-*co*-St)/HDTMA-MMT composite (Fig. 12).

Recovery of phenol

To test the adsorbent's reusability, hot water was used to rinse the poly (AA-co-St)/HDTMA-MMT-phenol. Fig. 16 shows that the maximum adsorbed amount of the phenol decreased from 150.7 mg/g to 140 mg/g after the 5th use. The desorption of phenol from the adsorbent using hot water was about 98.1 % in the first adsorption/desorption cycle and decreased significantly to 92.8 % after five cycles.

The composite's ability to absorb the phenol in water decreased by 5.2 %. The results demonstrate that in this study adsorbent might be reused at least five times.

CONCLUSIONS

In this study, the adsorption kinetic of phenol onto poly(AA-*co*-St)/HDTMA-MMT composite was investigated and the following conclusions can be obtained: The adsorption of the phenol increased with the initial concentration. The isotherm is of L-type. Adsorption equilibrium was achieved within 180 min. SEM micrographs of the adsorbent indicate that the
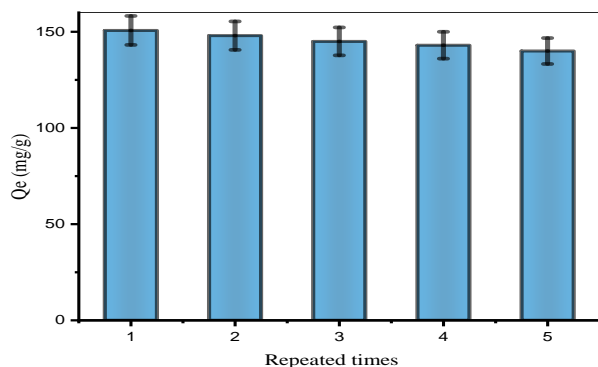
Fig. 16: Desorption cycles (initial concentration: 100 mg/L)

surface is heterogeneous and therefore offers better adsorption sites. The intercalation of poly(acrylic acid-co-styrene) into the interlayer space of montmorillonite is confirmed by XRD. Freundlich isotherm has a better fitting model than Langmuir as the former has a higher regression coefficient; thus indicating the heterogeneity of the composite's surface. The latter may also depend strongly on the chemical structure of phenol. The maximum amount of adsorption of phenol was determined using the Langmuir model; the latter model was found to be inadequate with the obtained experimental results with values reaching 150.7 mg/g. The adsorption data were modeled using the pseudo-first-order and pseudo-second-order kinetic equations. It was shown that adsorption kinetics can be well described by the pseudo-second-order equation. The observed adsorption phenomenon appears to be responsible for the hydrogen bonding, electrostatic interaction, and the hydrophobic interaction between phenol and the composite. All of these findings suggest that poly(AA-*co*-St)/HDTMA-MMT composite is an efficient adsorbent for phenol uptake in wastewater. The proprieties adsorptive of clay was improved by intercalation of poly(acrylic acid-co-styrene). Overall, the synthesized poly(AA-co-St)/HDTMA-MMT could be a promising adsorbent for the removal of phenol from polluted water.

Abbreviations

acrylic acid	AA
styrene	St
poly (acrylic acid-co-styrene)	poly(AA-co-St)
hexadecyltrimethyl ammonium bromide	HDTMABr
cetyltrimethylammonium bromide	CTAB
montmorillonite	MMT
poly (acrylic acid-co-styrene)/montmorillonite-hexadecyltrimethyl ammonium bromide	poly(AA-co-St)/HDTMA-MMT
polymethyl Methacrylate	PMMA
polypyrrole	PP
Fourier transform infrared spectroscopy	FTIR
X-ray diffraction	XRD
scanning electron microscopy	SEM
thermogravimetric analysis	TGA
UV-Vis spectrophotometry	UV-Vis
point of zero charge	pHpzc

REFERENCES

[1] Luz-Asunción M., Castaño V.M., Sánchez-Mendieta V., Velasco-Santos C., Martínez-Hernández A. L. Adsorption of Phenol from Aqueous Solutions by Carbon Nanomaterials of One and Two Dimensions: Kinetic and Equilibrium Studies, *J. Nanomater.*, **14**: 1-14. (2015).

[2] Yu J. Y., Shin M.Y., Noh J.H., Seo J.J., Adsorption of Phenol and Chlorophenols on Hexadecyltrimethylammonium and Tetramethylammonium-Montmorillonite from Aqueous Solutions, *J. Geosci.*, **8**: 191-198 (2004).

[3] Huang Y., Ma X. Y., Liang G. Z., Yan H. X., Adsorption of Phenol with Modified Rectorite from Aqueous Solution, *Chem. Eng. J.,* **141(3)**: 1–8 (2008).

[4] Villegas L.G.C., Mashhadi N., Chen M., A Short Review of Techniques for Phenol Removal from Wastewater, *Curr. Pollution Rep.*, **2**: 157–167 (2016).

[5] Kazemi P., Peydayesh M., Bandegi A., Mohammadi T., Bakhtiari O., Stability and Extraction Study of Phenolic Wastewater Treatment by Supported Liquid Membrane Using Tributyl Phosphate and Sesame Oil as Liquid Membrane, *Chem Eng Res Des.*, **92(2)**: 375–83 (2014).

[6] Sarkar M., Acharya PK., Use of Fly Ash for the Removal of Phenol and its Analogues from Contaminated Water, *J. Waste Manag.,* **26(6)**: 559-570 (2006).

[7] Noi N., Cam N., Thanh D., Hung T., Dinh B., Dae H., Synthesis of Organoclays and their Application for the Adsorption of Phenolic Compounds from Aqueous Solution, *J Ind Eng Chem*., **19(2)**: 640-644 (2013)

[8] Slimani M.S., Ahlafi H., Moussout H., Boukhlifi F., and Zegaoui O., Adsorption of Hexavalent Chromium and phenol onto Bentonite Modified With HexaDecylTriMethylAmmonium Bromide (HDTMABr), *JAC*, **8(2)**: 1602–1611 (2014).

[9] Vazquez G., Gonzalez-Alvarez J., Garcia A., Freire M. S., and Antorrena G., Adsorption of Phenol on Formaldehyde-Pretreated Pinus Pinaster Bark: Equilibrium and Kinetics, *Bioresour. Technol*., **98(8)**: 1535–40 (2007).

[10] Polat H., Molva M., Polat M., Capacity and Mechanism of Phenol Adsorption on Lignite, *Int. J. Miner. Process*., **79(4)**: 264–73 (2006).

[11] Ceylan Z., Mustafaoglu D., Malkoc E., Adsorption of Phenol by MMT-CTAB and WPT-CTAB: Equilibrium, Kinetic and Thermodynamic Study, *Part. Sci. Technol.,* **36(6)**: 716-726 (2018).

[12] Khodabakhsh S., Alaiee E., Taghavi L., Samiee L., Comparing Nanocomposites of TiO_2/SBA-15 and TiO_2/GO for Removal of Phenol out of Aqueous Solutions, *Iran. J. Chem. Chem. Eng. (IJCCE)*, **39(5)**: 121-130 (2020).

[13] Wang Y.Q., Gu B., Xu W.L., Electro-Catalytic Degradation of Phenol on Several Metal-Oxide Anodes, *J. Hazard. Mater.*,**162(3)**: 1159–64 (2009).

[14] Li M., Feng C., Hu W., Zhang Z., Sugiura N., Electrochemical DEgradation of Phenol Using Electrodes of Ti/RuO_2–Pt and Ti/IrO_2–Pt, *J. Hazard. Mater.*, **162(1)**: 455–62 (2009).

[15] Yang C., Qian Y., Zhang L., Feng J., Solvent Extraction Process Development and Onsite Trial-Plant for Phenol Removal from Industrial Coal-Gasification Wastewater, *Chem. Eng. J.,* **117(2)**: 179–85 (2006).

[16] Víctor-Ortega M.D., Ochando-Pulido J.M., Martínez-Ferez A., Performance and Modeling of Continuous Ion Exchange Processes for Phenols Recovery from Olive Mill Wastewater, *Process Saf. Environ. Prot.,* **100**: 242–51 (2016).

[17] Abdel-Ghani N.T., El-Chaghaby G.A., Helal F.S., Individual and Competitive Adsorption of Phenol and Nickel onto Multiwalled Carbon Nanotubes, *J. Adv. Res.,* **6(3)**: 405–15 (2015).

[18] Matthews T., Majoni S., Nyoni B., Naidoo B., Chiririwa H., Adsorption of Lead and Copper by a Carbon Black and Sodium Bentonite Composite Material: Study on Adsorption Isotherms and Kinetics, *Iran. J. Chem. Chem. Eng. (IJCCE)*, **38(1)**: 101-109 (2019).

[19] Anisuzzaman S. M., Bono A., Krishnaiah D., Tan Y. Z., A Study on Dynamic Simulation of Phenol Adsorption in Activated Carbon Packed Bed Column, *J. King Saud Univ. Eng. Sci.,* **28(1)**: 47–55 (2016).

[20] El-Sigeny S., Mohamed S.K., Abou Taleb M.F., Radiation Synthesis and Characterization of Styrene/Acrylic Acid/Organophilic Montmorillonite Hybrid Nanocomposite for Sorption of Dyes from, *Polym. Compos.,* **35(12)**: 2353-2364 (2014).

[21] Li G., Xu Q., ying X., Renchao J., Enhanced Adsorption and Fenton Oxidation of 2,4-Dichlorophenol in Aqueous Solution Using Organobentonite Supported nZVI, *Sep. Purif. Technol.,* **197**: 401-406 (2018).

[22] Cao Ch.Y., Meng L.K., Zhao Y.H., Adsorption of Phenol from Wastewater by Organo-Bentonite, *Desalin. Water Treat*., **52(21)**: 3504-3509 (2014).

[23] Mojoudi N., Mirghaffari N., Soleimani M., Phenol Adsorption on High Microporous Activated Carbons Prepared from Oily Sludge: Equilibrium, Kinetic and Thermodynamic Studies. *Sci. Rep*., **9**: 19352 (2019).

[24] Asnaoui H., Dehmani Y., Khalis M., Hachem E.K., Adsorption of Phenol from Aqueous Solutions by Na–Bentonite: Kinetic, Equilibrium and Thermodynamic Studies, *Int. J. Environ. Anal. Chem.,* **102(13)**: 3043-3057 (2020).

[25] Seyed A.H., Shervin D.A., Manouchehr V., Abdolreza S., Mohtada S., Green Electrospun Membranes Based on Chitosan/Amino-Functionalized Nanoclay Composite Fibers for Cationic Dye Removal: Synthesis and Kinetic Studies, *ACS Omega*, **6(16)**: 10816−10827 (2021).

[26] Hariani P., Riyanti F., Ratnasari H., Adsorption of Phenol Pollutants from Aqueous Solution Using Ca-Bentonite/Chitosan Composite, *J. Mns. Lingk*., **22(2)**: 233-23 (2015).

[27] Awad A.M., Shaikh Sh. M.R., Jalab R., Gulied M. H., Nasser M. S., Benamor A., Adham S., Adsorption of Organic Pollutants by Natural and Modified Clays: A Comprehensive Review, *Sep. Purif. Technol.,* **228**: 115719 (2019).

[28] Islam M.M., Biswas S., Hasan M.M., Haque P., Rimu S.H., Rahman M.M., Studies of Cr (VI) Adsorption on Novel Jute Cellulose-Kaolinite Clay Biocomposite, *Desal. Water Treat.,* **123**: 265–276 (2018).

[29] Bhattacharyya K.G., Gupta S.S., Adsorption of a Few Heavy Metals on Natural and Modified Kaolinite and Montmorillonite: A Review, *Adv. Colloid Interface Sci.*, **140(2)**: 114 (2008).

[30] Yu W.H., Li N., Tong D.S., Zhou C.H., Lin C.X.C., Xu C.Y., Adsorption of Proteins and Nucleic Acids on Clay Minerals and their Interactions: A Review, *Appl. Clay Sci.,* **80**: 443–452 (2013).

[31] Ngulube, T.; Gumbo, J.R.; Masindi, V.; Maity, A., An Update on Synthetic Dyes Adsorption onto Clay Based Minerals: A state-of-art Review, *J. Environ. Manage.,* **191**: 35 (2017).

[32] Hernández-Hernández K.A., Illescas J., Díaz-Nava M.C., Martínez-Gallegos S., Muro-Urista C., Ortega-Aguilar R., Rodríguez-Alba E., Rivera E., Preparation of Nanocomposites for the Removal of Phenolic Compounds from Aqueous Solutions, *Appl. Clay Sci*., **157**: 212-217 (2018).

[33] Ben Bouabdallah A., Djelali N., Study of the Effect of Various Parameters on the Adsorption of Heavy Metals by Bentonite-Polypyrrole Composite, *Iran. J. Chem. Chem. Eng.,* **342(3)**: 786-800 *(2023).*

[34] Hassan T., Salam A., Khan A., Khan S.U., Khanzada H., Wasim M., Khan M.Q., Kim I.S., Functional Nanocomposites and their Potential Applications: A Review, *J. Polym. Res.,* **28**: 36 (2021).

[35] Pavlidou S., Papaspyrides C.D., A Review on Polymer Layered Silicate Nanocomposites, *Prog. Polym. Sci.,* **33(12)**: 1119–1198 (2008).

[36] Zidan T.A., Synthesis and Characterization of Modified Properties of Poly (methyl Methacrylate)/Organoclay Nanocomposites, *Polym. Compos.,* **41(2)**:1–9 (2019).

[37] Anadão P., Polymer/clay Nanocomposites: Concepts, Researches, Applications and Trends for the Future, In: Ebrahimi, F. (Ed.), Nanotechnology and Nanomaterials "Nanocomposites - New Trends and Developments" INTECH, 1–16 (2012).

[38] Bergaya, F.; Lagaly, G. General Introduction: Clays, Clay Minerals, and Clay Science, In: Bergaya, F., Lagaly, G. (Eds.), "Handbook of Clay Science. Developments of Clay Science", Vol. 5. Elsevier, Amsterdam, Chp., **1**: 1–19 (2013).

[39] Bergaya, F.; Detellier, C.; Lambert, J.-F.; Lagaly, G. Introduction to clay-polymer Nanocomposites (CPN), In: Bergaya, F., Lagaly, G. (Eds.), "Handbook of Clay Science. Developments of Clay Science", Vol. 5. Elsevier, Amsterdam, Chp. **13**: 655–677 (2013).

[40] Zarei S., Ghasem R. B., Sadeghi M., Montmorillonite Nanocomposite Hydrogel Based on Poly (acrylicacid-co-acrylamide): Polymer Carrier for Controlled Release Systems, *Iran. J. Chem. Chem. Eng (IJCCE).*, **38(5)**: 31-43 (2019).

[41] Okada A., Kawasumi M., Usuki A., Kojima Y., Kurauchi T., Kamigaito O., In Polymer Based Molecular Composites, Schaefer, D. W., Mark, J.E., (Eds.), *MRS Symposium Proceedings, Materials Research Society: Pittsburgh*, **171**: 45–50 (1990).

[42] Lerari D., Peeterbroeck S., Benali S., Benaboura A., Dubois Ph., Combining Atom Transfer Radical Polymerization and Melt Compounding for Producing PMMA/Clay Nanocomposites, *J. Appl. Polym. Sci.,* **121(2)**: 1355–1364 (2011).

[43] Sanchez C., Belleville Ph., Popalld M., Nicole L., Applications of Advanced Hybrid Organic–Inorganic Nanomaterials: From Laboratory to Market, *Chem. Soc. Rev.*, **40**: 696-753 (2011).

[44] Azeez A., Rhee K., Park S., Hui D., Epoxy Clay Nanocomposites – Processing, Properties and Applications: A Review, *Compos. B: Eng.,* **45(1)**: 308-320 (2013).

[45] Bharadwaj R. K., Modeling the Barrier Properties of Polymer-Layered Silicate Nanocomposites, *Macromolecules,* **34(26)**: 1989–1992 (2001).

[46] Lerari D., Peeterbroeck S., Benali S., Benaboura A., Dubois Ph., Use of a New Natural Clay to Produce Poly (methylmethacrylate) -Based Nanocomposites, Polym. Int., **59(1)**: 71–77 (2010).

[47] Rahman M., Rimu S. H., Biswas S., Rashid T.U., Chisty A.H., Preparation of Poly (Acrylic Acid) Exfoliated Clay Composite by in-situ Polymerisation for Decolouration of Methylene Blue from Wastewater, *Int. J. Environ. Anal. Chem.*, **19**: 32-37 (2020).

[48] Wang L., Zhang J., Wang A., Fast Removal of Methylene Blue from Aqueous Solution by Adsorption onto chitosan-g-poly (Acrylic Acid) /Attapulgite Composite, *Desalination.* **266(3)**: 33 (2011).

[49] Gupta V.K., Agarwal S., Singh P., Pathania D., Acrylic Acid Grafted Cellulosic Luffa Cylindrical Fiber for the Removal of Dye and Metal Ions, *Carbohydr. Polym.*, **98(1)**: 1214-1221 (2013).

[50] Liu J., Liu G., Liu W., Preparation of Water-Soluble β-Cyclodextrin/Poly(Acrylic Acid)/Graphene Oxide Nanocomposites as New Adsorbents to Remove Cationic Dyes from Aqueous Solutions, *Chem. Eng. J.*, **257**: 299-308 (2014).

[51] Saberi A., Alipour E., Sadeghi M., Superabsorbent Magnetic Fe_3O_4-based Starch-poly (Acrylic Acid) nanocomposite Hydrogel for Efficient Removal of Dyes and Heavy metal Ions from Water, *J. Polym. Res.* **26**: 271 (2019).

[52] Huang G., Liang H., Wang X., Gao J., Poly (Acrylic Acid)/Clay Thin Films Assembled by Layer-by-Layer Deposition for Improving the Flame Retardancy Properties of Cotton, *Ind. Eng. Chem. Res.,* **51(38)**: 12299–12309 (2012).

[53] Wu T., Xie T., Yang G., Preparation of Exfoliated Polyacrylic Clay Nanocomposites with High Loading: An Investigation Into the Intercalation of Ammonium-Terminated Polyacrylic Acid and Polyacrylates, *J. Polym. Sci. B Polym. Phys.,* **46(21)**: 2335-2340 (2008).

[54] Zhang J., Wang L., Wang A., Preparation and Properties of Chitosan-G-Poly (Acrylic Acid)/Montmorillonite Superabsorbent Nanocomposite via in Situ Intercalative Polymerization, *Ind. Eng. Chem. Res.*, **46(8)**: 2497(2007).

[55] Moon H., Kook S.K., Park H.C., Adsorption of Phenols onto a Polymeric Sorbent, *Korean J. Chem. Eng.,* **8**: 168-176 (1991).

[56] Biswas S., Rashid T., Debnath T., Haque P., Rahman M., Application of Chitosan-Clay Biocomposite Beads for Removal of Heavy Metal and Dye from Industrial Effluent, *J. Compos. Sci.*, **16(4)**: 1-14 (2020).

[57] Bhatia M., Rajulapati S. B., Sonawane S., Girdhar A., Synthesis and Implication of Novel Poly (Acrylic Acid)/Nanosorbent Embedded Hydrogel Composite for Lead Ion Removal, *Scientific Reports,* **7**: 16413 (2017).

[58] Djamaa Z., Lerari D., Mesli A., Bachari K., Poly(acrylc acid-co-styrene)/Clay in a Nocomposites: Efficient Adsorbent for Methylene Blue Dye Pollutant, *Int. J. Plast. Technol.*, **23**: 110–121 (2019).

[59] Belalem K., Benaboura A., Lerari D., Kanoun N., Chebout R., Effect of Cationic and Anionic Clays as Supports for Styrene Polymerization Initiated by Metallocenes/MAO Catalytic System, *Polym. Bull.,* **77**: 4289-4305 (2020).

[60] Ferhat D., Nibou D., Mekatel E., Amokrane S., Adsorption of Ni^{2+} Ions onto NaX and NaY Zeolites: Equilibrium, Kinetics, Intra Crystalline Diffusion and Thermodynamic Studies, *Iran. J. Chem. Chem. Eng. (IJCCE),* **38(6)**: 63-81 (2019).

[61] Abdelwahab O., Amin N.K., Adsorption of Phenol from Aqueous Solutions by Luffa Cylindrica Fibers: Kinetics, Isotherm and Thermodynamic Studies, *Egypt. J. Aquat. Res.,* **39(4)**: 215–223 (2013).

[62] Kam W., Chiam-Wen L., Lim J. Y., Ramesh S., Electrical, Structural, and Thermal Studies of Antimony trioxide-doped Poly (Acrylic Acid)-Based Composite Polymer Electrolytes, *Ionics,* **20**: 665–674 (2014).

[63] Ltifi I., Ayari F., Chehimi B. D., Ayadi M. T. Physicochemical Characteristics of Organophilic Clays Prepared Using two Organo-Modifiers: Alkylammonium Cation Arrangement Models, *Appl. Water Sci.*, **8(91)**: 1-8 (2018).

[64] Banat F.A., Al-Bashir B., Al-Asheh S., Hayajneh O., Adsorption of Phenol by Bentonite, *Environ. Pollut.*, **107**: 391-398 (2000).

[65] Lin R.Y., Chen B., Suen Sh., Preparation of Porous Polymethyl Methacrylate/Organo-Montmorillonite Composite Membranes for Phenolic Compound Adsorption, *Sep. Sci. Technol.*, **46(3)**: 409-419 (2011).

[66] Giles C.H., Smith D., A General Treatment and Classification of the Solute Adsorption Isotherm I. Theoretical, *J. Colloid Interface Sci.*, **47(3)**: 755-765 (1974).

[67] Greluk M., Hubicki Z., Isotherm and Thermodynamic Studies of Reactive Black 5 Removal by Acid Acrylic Resins, *Chem. Eng. J.,* **162(3)**: 919-926 (2010).

[68] Yağmur H.K., Synthesis and Characterization of Conducting Polypyrrole/Bentonite Nanocomposites and In-Situ Oxidative Polymerization of Pyrrole: Adsorption of 4-Nitrophenol by Polypyrrole/Bentonite Nanocomposite, *Chem. Eng. Commun.*, **207(8)**: 1171-1183 (2020).

[69] Calace N., Nardi E.B., Petronio M., Pietroletti M., Adsorption of Phenols by Papermill Sludges, *Environ. Pollut.,* **118(3)**: 315–319 (2002).

[70] Li Y., Du Q., Liu T., Equilibrium, Kinetic and Thermodynamic Studies on the Adsorption of Phenol onto Graphene, *Mater. Res. Bull.*, **47(8)**: 1898–1904 (2012).

[71] Djamaà Z., Benabadji K. I., Choukchou-Braham E., Mansri A., Removal of Hexavalent Chromium from Aqueous Solutions Using N-octyl Quaternized Poly(4-vinylpyridine): Kinetic and Equilibrium Studies, *J. Macromol. Sci. - Pure Appl. Chem.,* **50(7)**: 679-684 (2013).

[72] Bulut Y., Karaer H., Removal of Methylene Blue from Aqueous Solution by Crosslinked Chitosan-G-poly (Acrylic Acid) / Bentonite Composite, *Chem. Eng. Commun.*, **202(12)**: 1635-1644 (2014).

[74] Esmaeili H., Foroutan R., Adsorptive Behavior of Methylene Blue onto Sawdust of Sour Lemon, Date Palm, and Eucalyptus as Agricultural Wastes, *J. Disper. Sci. Technol.,* **40(7)**: 990-999 (2018)

[75] Abshirini Y., Foroutan R., Esmaeili H., Cr(VI) Removal from Aqueous Solution Using Activated Carbon Prepared from Ziziphus Spina-Christi Leaf, *Mater. Res. Express.,* **6(4)**: 1-37 (2019).

[76] Lagergren S.K., About the Theory of So-called Adsorption of Soluble Substances Sven, *Vetenskapsakad. Handingarl*, **24**: 1 (1898).

[77] Ho Y.S., McKay G., Pseudo-Second Order Model for Sorption Processes, *Process Biochem.*, **34(5)**: 451-465 (1999).

[78] Karadağ E., ÖB Ü., Saraydin D., Swelling Equilibria and Dye Adsorption Studies of Chemically Crosslinked Superabsorbent Acrylamide/Maleic Acid Hydrogels, *Eur. Polym. J.*, **38(11)**: 2133-2141 (2002).

[79] Abdel-Ghani N.T., El-Chaghaby G.A., Helal F.S., Individual and Competitive Adsorption of Phenol and Nickel onto Multiwalled Carbon Nanotubes, *J. Adv. Res.*, **6(3)**: 405-415 (2014).